Click to view PDF-Slide presentation

Complex Petrophysical Studies to Evaluate the Safety of an Underground Gas Storage in Porous Rocks*

Carlo Dietl[1], Roland Braun[2], Hansjörg Baumgartner[1], Eberhard Jahns[1], and Tobias Rudolph[3]

Search and Discovery Article #80642 (2018)**
Posted August 20, 2018

*Adapted from extended abstract prepared in conjunction with oral presentation given at AAPG 2018 AAPG Annual Convention and Exhibition, Salt Lake City, Utah, May 20-23, 2018

[1]Gesteinslabor Dr. Eberhand Jahns, Heiligenstadt, Germany (dietl@gesteinslabor.de)
[2]Dr. Roland Braun - Consultancy in Rock Mechanics, Schwielowsee, Germany
[3]Uniper Energy Storage GmbH, Essen, Germany

Abstract

Underground storage of natural gas plays a decisive role for the reliability of energy supply. In this context the integrity of the reservoir and its seal is essential.

We are currently investigating a former natural gas reservoir as possible pore space underground gas storage with respect to the safety of the structure. The reservoir is situated within the eastern part of the Bavarian Molasse Basin (Germany). To check the stability and tightness of the storage strength, in situ stresses and in situ threshold pressure measurements were carried out on drill core material from an exploration well. The core covers the reservoir and its seal. Our investigations are completed by cyclic compressibility tests to get insight into the poroelastic behaviour and its change with cyclic loading/unloading of the reservoir rock and the seal. The compressibility tests are part of the joint scientific-industrial research storage safety project SUBI.

The seal is a smectite-rich clayey to silty marlstone. Its porosity is in average 2 %. Threshold pressure measurements gave values between 10 and 15 MPa pointing to a brine permeability of 10^{-7} mD. The reservoir consists of fine grained sandstone and calcareous marl. Its porosity scatters due to lithological differences between 3 and 33 %. Gas permeability varies as a function of porosity between 10^{-1} to 10^{3} mD.

In situ stresses were investigated in 3D on drill core material from the seal marlstone and the reservoir sandstone with the RACOS® (Rock Anisotropy Characterisation On Samples) method (e.g. Braun et al., 2000; Braun and Reinhold, 2017). Additionally, the changes of in situ stresses with increasing pore pressure were determined. The main principal total stress equals the vertical overburden pressure, while the high pore pressure effectiveness in the sandstone leads to a significantly lower effective vertical stress in the reservoir. The main horizontal effective and total stresses are oriented NNW-SSE to N-S as a result of the alpine orogenesis.

Both, seal and reservoir rock are weakest perpendicular to an E-W trending fault zone and show signs of ductile failure.

The combination of stress and strength data let us assume a high stability of the storage system. Even leakage due to a high gas injection pressure is unlikely due to the relatively high threshold pressure in the range between 10 and 15 MPa.

The cyclic compressibility tests indicate mainly two things: (1) the cyclic loading and unloading does not change the poroelastic behaviour of the reservoir sandstone and (2) the reservoir sandstone does not seem to record the cyclic loading/unloading history. Consequently, we recommend for compressibility testing to carry out several testing cycles for the determination of the compressibility moduli.

Threshold pressure tests before and after cyclic loading/unloading of caprock specimens will prove if frequent depletion and inflation of a porous gas storage has an impact on the storage seal and influences negatively the stability and integrity of the storage system.

1. Introduction

Energy safety is an important topic for modern societies. This needs a guaranteed access to base load capable energy sources such as geothermal heat, natural gas, or coal. One of the main points in advanced energy application concepts is energy storage, which can serve as a measure to allow energy gained by intermittent techniques to provide base load power. One example for such a strategy is “power to gas”: electricity produced from wind turbines is used to produce hydrogen by electrolysis from water; the hydrogen is then allowed to react with CO_2 in a process called methanation to produce methane or “artificial” natural gas. Of course, not only wind energy can be stored by this method, but all other kind of electrical power. Nevertheless, it is ecologically and economically most worthwhile to transfer intermittent electrical power – such as wind and solar energy – into base load energy, i.e. methane.

This methane can be stored like natural gas in salt cavern, aquifer or pore space storages. Different from usual gas storages whose gas content serves as heat source and which are filled in summer and depleted during winter, “power to gas” storages whose gas will serve as electrical power source will be filled and emptied much more frequently. This, of course, means stress to the reservoir and its caprock. The frequent and cyclic inflation and depletion of gas storages may change its poroelastic properties plus the tightness of the caprock which are crucial for the safety and integrity of the storage. Therefore, the interdisciplinary and joint scientific project SUBI was initiated to investigate the integrity and safety of gas storages. Gesteinslabor Dr. Eberhard Jahns does within this framework two types of long term laboratory tests: (1) cyclic compressibility tests on reservoir sandstone, and (2) threshold pressure tests before and after numerous depletion-inflation cycles on a clayey to silty marlstone which acts as caprock.

Here we present the first results from the cyclic compressibility tests on the reservoir sandstone. The chosen storage site is situated in Southern Germany within the Bavarian Molasse Basin. The storage is well known from its rock physical and geomechanical parameters, since we also carried out porosity and permeability measurements as well preliminary threshold pressure measurements and in situ 3D stress determinations with the RACOS® method as part of a previous project. The methods applied, and results achieved from this prior study are also presented below.

2. Methodology

2.1. Mineral Analysis by X-ray Diffractometry (XRD) and Infrared Spectroscopy (FTIR)

Semi-quantitative determination of the mineral composition of three caprock samples was done by combined XRD and FTIR measurements. XRD analyses were done with and a BRUKER D2 PHASER diffractometer. The infrared spectra were recorded in transmission mode between 4000 and 400 cm^{-1} with a Mattson 3000 type Fourier transform infrared spectrometer. The data analysis and evaluation of the XRD and IR diagrams was done manually according to mineralogical standard methods. The combination of the two methods, namely XRD and FTIR, allows for a standard deviation of < 10 weight-% of the amount of the individual mineral phases.

2.2. Density and Porosity Measurements

Bulk densities ρ_B of all specimens were calculated using their dimensions and respective weight following the ISRM (1977). Bulk densities were determined on oven dried samples. The grain volume was determined with a helium pycnometer (Micromeritics AccuPyc II 1340) under ambient conditions. This device measures the overall sample volume after Boyle's law. The porosity is determined basically as the ratio between bulk density and grain density.

2.3. Gas Permeability

Investigations were carried out with a semiautomatic device (provided by GL Test Systems) under ambient conditions. The flow rate is determined with two thermal mass flow meters within two metering ranges of 10 sccm (standard cubic centimetre) and 100 sccm, respectively. The determined permeability data were recalculated applying a Klinkenberg correction according to Rieckmann (1970).

2.4. Threshold Pressure

Usually at Gesteinslabor we follow the modified continuous injection method developed by Meyn (1999) in a slightly modified manner. Applying this technique, we measure both, brine permeability and capillary threshold pressure of the storage caprock under in situ conditions. For a detailed description of the experimental setup and testing procedure see Dietl et al. 2014.

Due to the very delicate nature of the caprock material a modification and simplification of the continuous injection method was necessary. The high amount of smectite (see section 3.1) which started to swell when in contact with the formation water made a determination of the threshold pressure according to the method by Meyn (1999) impossible and no interpretable results could be achieved.

However, by applying a gas pressure onto the end face of an *unsaturated* cylindric specimen it can be detected directly if gas is intruding into the sample at the applied gas pressure. This test type is significantly less time consuming than the Meyn method and can therefore be repeated easily at various gas pressures. By this measure the threshold pressure can be ranked within a pressure interval which is generally sufficient for the evaluation of the seal capacity of the caprock. The applied method yields a careful and conservative threshold pressure estimate, because the specimen might be unsaturated, and the entire differential pressure operates over the entire specimen.

2.5. The RACOS® Procedure

RACOS® is a method for the determination of the 3D in situ stress field on drill core samples based on ultrasonic velocity investigations. P- and S-wave measurements are carried out on five to seven cubic specimens of minimum 1-inch edge length taken from a geographically reoriented homogeneous core section. V_P and V_S are measured in 15 to 21 directions under increasing isotropic pressure from atmospheric conditions to 200 MPa. With increasing isotropic pressure microcracks within the rock specimen induced by core removal from the in situ stress field are closed and, consequently, ultrasonic velocities rise.

The reversal of the coring-related loosening is shown by directional loading-related changes in the propagation velocity of elastic waves. Observed sudden changes in azimuth and dip of the principal velocity components during increases in loading indicate the opening/closure of cracks/micro-cracks. When these changes occur close to the anticipated recent effective in-situ stress at the time of coring, it can be assumed (after making appropriate checks) that there was a direct unloading effect, which was compensated by the reloading. In this way the principal effective in situ stress components can be derived directly from the load-dependent propagation directions of compressional waves before crack closure.

Since P- and S- waves propagate anisotropically through the rock, the velocity ellipsoid for both wave types, the ellipsoid of the Young's modulus and the ellipsoid of the rock compressibility can be calculated.

Based on these data the anisotropic pore pressure effectiveness (Biot coefficient) can be calculated. The direction of the least pore pressure effectiveness represents the preferred flow direction.

The so far achieved data (plus the pore pressure) allow the determination of the effective and total in situ stresses plus the recent and paleo tectonic stresses within the analysed formation.

In case strength data exist, the 3D stress data can be applied for borehole and formation stability calculations.

2.6. Compressibility Testing

2.6.1. Introduction

As stated in section 1 it is the aim of the compressibility tests to find out if the cyclic filling and emptying of the pore space of a cylindrical specimen, which acts as analogue for a pore space gas storage, changes its poroelastic characteristics.

The testing procedure consists of a sequence of three test types, which are described in detail below. A CPV test (see section 2.6.3) is followed by a depletion test (see section 2.6.4) and a so-called aging procedure (see section 2.6.5) which is aimed to weaken the specimen. Subsequently, a second CPV test and a second depletion test follow. So far three specimens S01, S02, and S03 were tested: In case of specimen S03 the second depletion test was skipped for technical reasons.

2.6.2. Test Equipment

The compressibility tests were carried out on a digitally controlled servo hydraulic testing machine with a maximum load range of 600 kN (accuracy class 1). The two-channel controller also operates an electromechanical pressure generator capable of providing the confining pressure of up to 200 MPa (accuracy class 0.5). The specimens are mounted in a triaxial cell with exchangeable pistons, provided by GL Test Systems. The pistons are perforated to provide drained conditions. True axial (mean of three LVDTs) and radial deformation of the sample (diametric with a strain gauge) are measured "in-vessel" to avoid the load frame deformation being included in the results of the deformation of the specimen. To avoid friction artefacts, the axial load is measured with an in-vessel load cell. Moreover, a hydrostatic pressure platen was used. The sample is situated within a semi-rigid NBR sleeve. Measurements of the radial deformation are not affected by the hose, because the strain gauge is attached directly to the specimen via steel buttons which are integrated into the NBR sleeve. No spherical seats are used. All the important parameters are recorded automatically; generally, with a recording interval of 5 s. The pore pressure is generated with a Quizix Q5200 syringe high precision metering pump system. This electromechanical pump is a high-pressure syringe pump that provides truly pulse-free pumping at very high precision and accuracy. Because all wetted parts are made of Hastelloy® C-276, brine and highly corrosive fluids can be handled directly. To avoid metering errors caused by temperature fluctuations, the whole pump system is situated in a mobile conditioning cabinet. The applied pore fluid corresponds to the formation brine within the investigated reservoir.

2.6.3. CPV Testing Procedure

During the CPV test a saturated and equilibrated specimen is exposed to increasing hydrostatic confining pressures P_c, in the present case at five P_c levels, namely 5, 10, 15, 20 and 26.3 MPa (see Figure 1a). The test is done under drained conditions at a pore fluid pressure P_p of 0.5 MPa. The final P_c step corresponds to the mean effective stress within the investigated pore gas storage. At all five P_c levels the expelled pore fluid volume and the volume strain of the specimen are measured to determine the pore space compressibility c_{pc} and bulk compressibility c_{bc} under hydrostatic conditions.

2.6.4. Depletion Tests: Testing Procedure

The CPV test is followed by the depletion test during which pore pressure P_p (max. 16.3 MPa; equaling the initial in situ P_p within the investigated reservoir), axial load S1 (max. 42 MPa; as determined from RACOS® for the investigated reservoir; see section 3.6) and radial confining pressure S3 (max. 37.5 MPa; as determined from RACOS®; see section 3.6) are varied as depicted in Figure 1b for the determination of the following poroelastic parameters:

1. the grain compressibility c_g (determined at the beginning of the test and with simultaneously increasing P_p, S1 and S3;

2. the bulk compressibility c_{bc} with changing all side confining pressure (S1 plus S3) and constant P_p (similar to c_{bc} as determined from the CPV test; from c_g and c_{bc} the Biot coefficient α can be calculated as: $\alpha = 1 - \frac{c_g}{c_{bc}}$)
3. the bulk compressibility c_{bp} at constant all side confining pressure (and changing pore fluid pressure which is increased temporarily from 16.3 MPa to 20 MPa)
4. the uniaxial pore space compressibility c_{pp} (at changing P_p). For this purpose, the pore fluid pressure is reduced from 16.3 MPa to 1 MPa at constant axial load. Since we aim to simulate reservoir depletion and related subsidence, we keep radial strain at zero (by a freely floating radial confining pressure S3 following basically the decreasing pore fluid pressure) and all deformation is accomplished and compensated by the axial strain. In a second step the pore fluid pressure is raised again from 1 MPa to 16.3 MPa, still keeping the axial load S1 constant at 42 MPa (slightly different for specimens S02 and S03; see section 4) and S3 free floating to allow all deformation being compensated by axial strain alone ($\varepsilon_r = 0$)
5. the horizontal depletion constant γ as the axial strain in response to changing P_p (also determined at the same depletion stage as c_{pp})
6. the constant compaction coefficient c_m as the ratio between S3 and P_p (also determined at the same depletion stage as γ and c_{pp})

2.6.5. Aging Cycles: Procedure

After the first CPV test and the first depletion test so-called aging cycles are carried out. For this purpose, similar depletion-inflation cycles are run as during the last part of the depletion test: the pore pressure is reduced from 16.3 MPa to 1 MPa and later on increased again to 16.3 MPa, axial load S1 is held constant at 42 MPa (slightly different for specimens S02 and S03; see section 4) and no radial strain is allowed. This measure simulates emptying and subsequent refilling of porous gas storage. Generally, 21 depletion-inflation cycles were done (see Figure 1c). Under current circumstances (i.e. emptying pore space gas storage during summer and replenishing it during winter) 21 years of storage operation are simulated.

3. Results

3.1. Results of the Mineral Analyses and Rock Composition

From optical inspection the caprock is classified as marl, while the reservoir rock can be described as fine grained sandstone.

The quantitative combined XRD/FTIR X-ray analysis of three caprock samples yielded an elevated amount (roughly 30 wt-%) of swellable three-layer clay minerals as smectite and mixed illite smectite. This make the marl mobile and instable.

3.2. Bulk and Grain Density

All together 120 specimens were investigated for their density, porosity, and permeability during the previous study named in section 1.

The bulk density of the caprock lies between 2.42 and 2.47 g/cm^3 around a mean of 2.44 g/cm^3. Within the reservoir the spread is wider. Bulk density ranges from 1.78 to 2.69 g/cm^3, the average reservoir sandstone has a bulk density of 2.07 g/cm^3.

The grain density of the caprock lies constantly between 2.71 and 2.74 g/cm^3 (average: 2.72 g/cm^3).

Reservoir grain density data scatter between 2.62 and 2.81 g/cm^3 around an average of 2.70 g/cm^3.

3.3. Results of the Porosity Measurements

The porosity data correlate well with the bulk density. The values for the caprock samples lie between 0.5 % and 3.60 % with a mean of 0.19% The reservoir values scatter wider between 3.10 and 33.40 % around an average of 23.2 %.

3.4. Results of the Gas Permeability Measurements

Gas permeability was only determined for the reservoir sandstone (101 samples). The gas permeability of the reservoir sandstone, scatters between $1.41*10^{-3}$ mD and $2.72*10^3$ mD (mean: $5.07*10^2$ mD).

3.5. Results of the Threshold Pressure Measurements

Due to some technical problems with the very soft caprock marl the successful threshold pressure tests were done with the simplified method described above (section 2.4). For this purpose, the end faces of the two successfully investigated specimens were pressurized with nitrogen at three gas pressure levels: 10 MPa, followed by 20 MPa, and finally 15 MPa. At a gas pressure of 10 MPa the gas flow into the specimens ceases after 37 to 50 h, because the nitrogen was not able at that entry pressure to percolate the marl sample. Different at the other two pressure levels: at 15 and 20 MPa a continuous gas flow was observed. Our interpretation is that the capillary threshold pressure is > 10 MPa and < 15 MPa. Applying some correlation calculations between threshold pressure and brine permeability (Ibrahim et al., 1970; Davies ,1991; and Dietl et al., 2014) we were able to estimate a brine permeability of roughly 10^{-7} mD.

3.6. RACOS® Results, Rock Strength, and Stability

RACOS® measurements were done to shed more light on the stability and tightness of the investigated pore space gas storage when raising the gas pressure within the reservoir from initial conditions. For this purpose, not only the in situ stresses in 3D were determined, but also the pore pressure dependency of the in situ stresses and the pore pressure effectiveness (also in 3D).

Investigations were done for a fine grained reservoir sandstone with an initial porosity of 14.1 % and a marly caprock with an initial porosity of 1.6 %. In both investigated lithologies the main compressive stress S1 acts vertically ($S1 = S_V$) and equals approximately the overburden pressure of roughly 42 MPa. The direction of the maximum compressive horizontal stress S_{HMAX} is – obviously as a result of the alpine orogeny – NNW-SSE, with a magnitude significantly smaller than S_V. The mean total horizontal stress in both layers is ca 37-38 MPa. The envisaged pore pressure increase due to inflation of the gas storage leads to a decrease in effective stresses (and consequently to an approximation towards failure) in particular in the reservoir itself and most efficiently under all side free deformation. Minimum strength for both lithologies was determined to be arranged horizontally and perpendicular to an E-W trending fault zone but in direction of the maximum compressional velocity. The lowest strength was observed in the marl which displays a mainly ductile failure behavior.

Joining strength and stress data allows for analyzing the stability situation under initial loading and with increased pore pressure within the reservoir and the caprock. This analysis indicates for all investigated situations a high stability. This is true for both, the compact/intact rock mass, as well as for the E-W trending steep fault. Even if the increased pore pressure is at first only active in the fault zone, the stability reserve is still high. This finding is the result of the low stress deviators at all investigated load configurations. It can be concluded that the envisaged pore pressure raise does not cause any mechanically induced leak in the undeveloped rock mass.

3.7. Results of the Compressibility Tests

3.7.1. Results of the CPV Tests

As explained above two CPV tests were carried out on each sample. Between both CPV tests lie one depletion test and an aging period of one week with 21 depletion/inflation cycles equaling a gas storage usage time of 22 years under current application conditions of a porous gas storage (the depletion test contains also one depletion/inflation cycle). The aging is not reflected in the poroelastic parameters. Although bulk volume strain and pore volume strain both change from CPV test 1 to CPV test 2, reflecting consolidation of the investigated three specimens, the poroelastic parameters bulk compressibility c_{bc} and pore volume compressibility (c_{pc}) do not differ strongly when comparing the results of both CPV tests (see Figure 2). In particular c_{bc} remains basically unchanged from one test to the other.

3.7.2. Results of the Depletion Tests

As for the CPV tests there lies one week of experimental aging in between both depletion tests: basically 21 aging cycles plus one CPV test; equaling 22 years of gas storage usage under the current conditions (storage depletion during winter and storage inflation during summer). The results are summarized in Figure 3. Besides for the first depletion test of specimen S01 we do not observe a strong consolidation as for the CPV tests. Also, almost none of the determined poroelastic parameters change from depletion test 1 to 2. The only exception is grain compressibility in case of specimen S01 which decreases by 20 %. Consequently, for this sample also the Biot coefficient changes: it increases from depletion test 1 to depletion test 2 from 0.68 to 0.74.

3.7.3. Aging Results

Since the aging cycles follow the same stress strain path as the last part of the depletion tests with its strong reduction and subsequent raise in pore pressure (see Figure 1b and Figure 1c), they can also be used for the calculation of several poroelastic parameters, namely c_m, (see Figure 3f) c_{pp} and γ. Our investigations show that equilibrium is reached after the first aging cycle; this means that the axial strain scatters only slightly from one cycle to the other and that the slope of the linear regression beam for each individual pore pressure vs. axial strain diagram (Figure 3f) does not change a lot from one depletion/inflation cycle to the next one: for sample S01 the constant compaction coefficient scatters between $8.81*10^{-5}$ and $9.79*10^{-5}$ MPa^{-1}, in case of specimen S02 c_m fluctuates between $1.55*10^{-6}$ and $2.37*10^{-6}$ MPa^{-1} and in case of sample S03 the compaction coefficient ranges between $2.82*10^{-6}$ and $3.80*10^{-6}$ MPa^{-1}. Only the first depletion branch yields significantly steeper regression beams with c_m values of $1.96*10^{-4}$ MPa^{-1} (specimen S01) $4.32*10^{-6}$ MPa^{-1} (specimen S02) and $6.13*10^{-6}$ MPa^{-1} (specimen S03). Apparently, also during aging first equilibrium has to be reached before reproducible poroelastic parameters can be generated. Application of this observation to the depletion tests (Figure 3e) shows that also here the depletion branch yields much greater compaction coefficients than the inflation branch, indicating that during depletion equilibrium is not yet reached and that only the inflation branch gives realistic and reproducible c_m values. Consequently, to determine a trustworthy compaction coefficient it is recommendable to run several depletion/inflation cycles. Simultaneously, more resilient pore volume compressibility data and depletion constant values are defined.

3.7.4. Summary of the compressibility testing results

In summary it can be stated from the so far carried out compressibility tests that none of the important poroelasticity parameters changes significantly due to the depletion/inflation aging cycles. Further tests will be necessary to verify this observation.

In particular, the aging cycles and the comparison of the compaction coefficients show that an extended consolidation phase and repetitive tests are indispensable to gain reliable, resilient compressibility data.

4. Discussion and Conclusions

We investigate a possible pore space gas storage in Southern Bavaria for its safety and integrity based on rock physical and geomechanical data. The storage consists of fine grained sandstone with variable porosity between 3 and 33 % and permeability in the wide range from 10^{-3} to $3*10^{3}$ mD as reservoir rock overlain by marly caprock with an average porosity of 0.19 % and a probable brine permeability of 10^{-7} mD.

The caprock permeability is only an estimate based on threshold pressure/permeability correlations (Ibrahim et al., 1970; Davies, 1990; and Dietl et al., 2014), because the soft nature of the marl prohibited the application of the routine technique at Gesteinslabor for combined brine permeability/threshold pressure measurements. The reason for the softness and mobility of the caprock, in particular under saturated conditions, is the abundance of swellable clay minerals such as smectite. A simplified method had to be applied which waives the necessity to work with saturated specimens. The simplified technique as described in section 2.4 does not guarantee full saturation of the specimen; moreover, the entire differential (gas) pressure acts on the whole specimen. Therefore, the result of the threshold pressure measurement represents a minimum and a conservative estimate of the capillary threshold pressure. Nevertheless, the threshold pressure investigations yielded a reasonable result: a capillary threshold pressure of > 10 and < 15 MPa close to the initial gas pressure within the reservoir of 16.3 MPa.

Based on these results for the sensitivity of the caprock to gas percolation the security estimations for the gas storage were broadened by also investigating the integrity and stability of the entire gas storage system and its sensibility to failure. For this purpose, RACOS® tests were carried out to determine in situ stresses in 3D and the pore pressure effectiveness (also in 3D) at initial conditions and at an increased pore pressure. The overall stress field reflects the alpine orogeny with an NNW-SSE directed S_{HMAX}, the maximum principal stress S1 is oriented vertically. The weakest points within the entire reservoir/caprock system are (1) the swelling capacity of the marly caprock which make it a highly ductile deformation behavior. and (2) an E-W trending fault zone which crosscuts the gas storage. However, our combined stress/strength data show that even at an elevated pore pressure and consequently reduced effective stresses the stability neither of the reservoir sandstone, nor of the marly seal reaches criticality.

Currently, we are occupied with question of material fatigue due to the repeated emptying and refilling of the reservoir. To approach this problem, we carry out cyclic compressibility tests on the reservoir sandstone and measure the poroelastic moduli and parameters. Of course, we observe with ongoing testing and deformation a consolidation of the so far tested three specimens expressed by relative high strain values during the first deformation cycles and decreasing strain data for the subsequent CPV and depletion tests. The strongest consolidation effects occurred for specimen S01 (see Figure 3). In this case we kept S1 constant at 42 MPa during all depletion/inflation cycles, irrespective, if doing depletion testing or carrying out the aging procedure. In contrast, depletion testing and aging of specimens S02 and S03 were done with a constant differential stress and a variable S01; this led to less consolidation and significantly smaller compaction coefficients compared to sample S01 (see Figure 3e). However, so far, we did not observe dramatic changes in the poroelasticity of the reservoir sandstone. The only exception is grain compressibility in case of specimen S01 which decreases by 20 % from depletion test 1 to depletion test 2. This is a surprising finding, because we would not expect the grain compressibility to change; rather we would anticipate this key number to be the most stable one. On the other hand, grain compressibility is – of all investigated poroelastic parameters – most sensitive to measurement errors. With the decreasing grain compressibility for specimen S01 also the Biot coefficient changes and – because bulk compressility basically stays constant – increases, i.e. the pore pressure effectiveness gets higher with ongoing testing and consolidation. This result seems to be contradictory with the expected and needs to be verified or falsified with further compressibility tests on more samples.

Another important finding of our so far investigations is the fact that even the most intense consolidation is not entirely recorded by the reservoir sandstone. This gets clear when we look at the first depletion branch of the aging cycles and the depletion branch of the depletion tests (see Figure 3e and Figure 3f): the build-up of axial strain during this first depletion is always much stronger as for the other depletion and inflation branches; consequently, also the constant compaction coefficient is in average twice as high as for the other depletion/inflation cycles. It seems as if some consolidation is always necessary to make the rock "remember" the deformation it already experienced. Therefore, we recommend strongly to carry out several depletion/inflation cycles (may it be as aging procedure or simply as depletion test) for correct c_m determination. Since the total radial stress and the normalized pore volume are not as consolidation sensitive as the axial strain (see Figure 3c and Figure 3d) they do not change that strongly from depletion cycle 1 to the following depletion/inflation cycles. Nevertheless, repeated depletion/inflation improves also in this case the data base.

We will continue with further cyclic compressibility tests to verify the so far achieved results. Moreover, we are going to test if the caprock is sensitive to poroelastic material fatigue by starting combined threshold pressure measurements and cyclic compressibility tests on the marly seal of the investigated pore space gas storage.

Our investigations show that the occupation with gas storage systems is a complex matter and that in particular the caprock is a delicate material which has to be handled with care. Moreover, we were able to show that a combined approach with several methods and investigating different aspects of the integrity of a pore space gas storage is necessary to prove its safety and longevity. The investigated storage example seems to be save and integer in terms of gas percolation and reservoir/seal fracturing, as long as the gas entry pressure does not exceed dramatically the initial gas pressure. Moreover, poroelastic fatigue seems to be improbable. Nevertheless, the currently gained data have to be double-checked and proven by further research.

Acknowledgements

This research is funded by the German Federal Ministry of Education and Research within the framework program "Geo:N – Geosciences for Sustainability" under support code 03G0869F.

References Cited

Braun, R., E. Jahns, and D. Stromeyer, 2000, Verfahren zur Bestimmung der raumlichen Gesteins- und Gebirgsanisotropie sowie des Gebirgsspannungszustandes an Probekorpern: Patent specification DE 198 30 196 C2, issued patent No. 198 30 196, registered 06/07/1998, issued 30/11/2000.

Braun, R., and C. Reinhold, 2017, Ermittlung von 3D-Gebirgsspannungszustanden fur den Brenner Basistunnel: Geotechnik, v. 40, p. 250-264.

Davies, P.B., 1991, Evaluation of the Role of Threshold Pressure in Controlling Flow of Waste-Generated Gas into Bedded Salt at the Waste Isolation Pilot Plant (WIPP): Sandia Report, SAND 90-3246, 62 p.

Dietl, C., H. Baumgartner, and E. Jahns, 2014, Underground Storage and Its Caprock: The Good Cap / Bad Cap Principle: DGMK-Tagungsbericht 2014-1, p. 355-364.

Egermann, P., J.M. Lombard, and P. Bretonnier, 2006, A Fast and Accurate Method to Measure Threshold Capillary Pressures in Caprocks Under Representative Conditions: Paper SCA A46, International Symposium of the Society of Core Analysis, Trondheim, Norway, 14 p.

Ibrahim, M.A., M.R. Tek, and D.L. Katz, 1970, Threshold Pressure in Gas Storage: American Gas Association, Inc., Arlington, Virginia, 309 p.

ISRM, 1977, Suggested Methods for Determining Water Content, Porosity, Density, Absorption, and Related Properties and Swelling and Slake-Durability Index Properties: International Society for Rock Mechanics, p. 141-151.

Meyn, V., 1999, Die Bedeutung des Sperrdruckes (Threshold Pressure) fur den Fluidtransport in niedrigstpermeablen Gesteinen: Experimentelle und theoretische Aspekte: DGMK-Tagungsbericht 1999-1, p. 255-264.

Rieckmann, M, 1970, Untersuchung von Turbulenzerscheinungen beim Fliesen von Gasen durch Speichergesteine unter Berucksichtigung der Gleitstromung: Erdol-Erdgas-Zeitschrift, v. 86 p. 36-51.

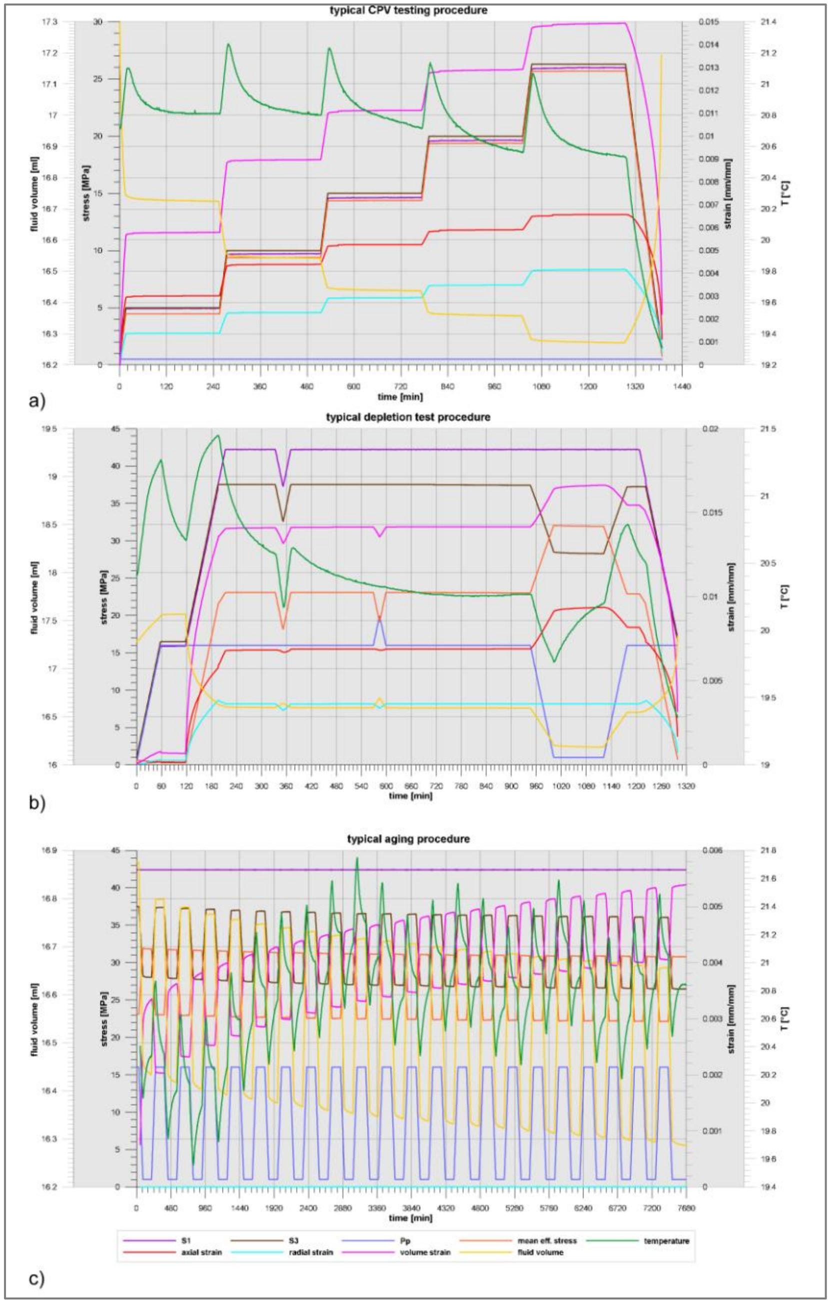

Figure 1. Typical metering cycle for a) a CPV test; b) a depletion test; and c) the aging procedure. All three testing stages are combined as described in section 2.6.1.

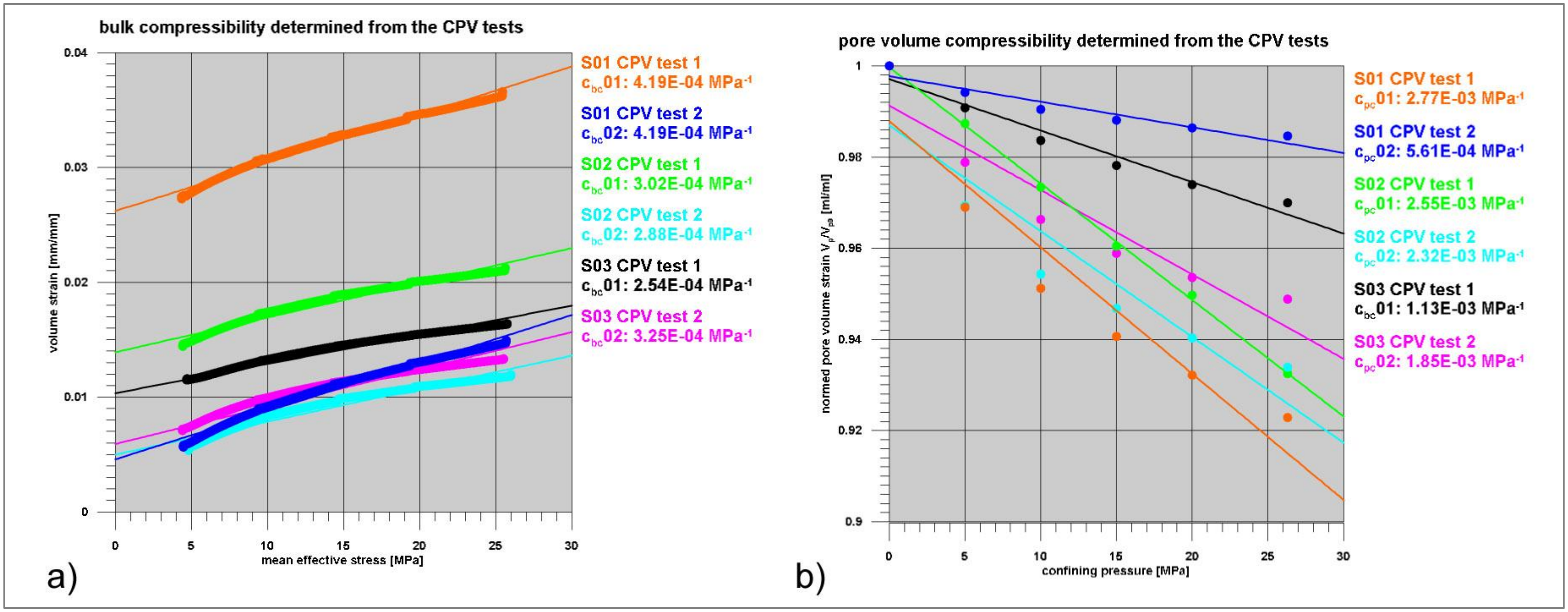

Figure 2. Poroelastic parameters as determined from the CPV tests: a) bulk compressibility; b) pore volume compressibility.

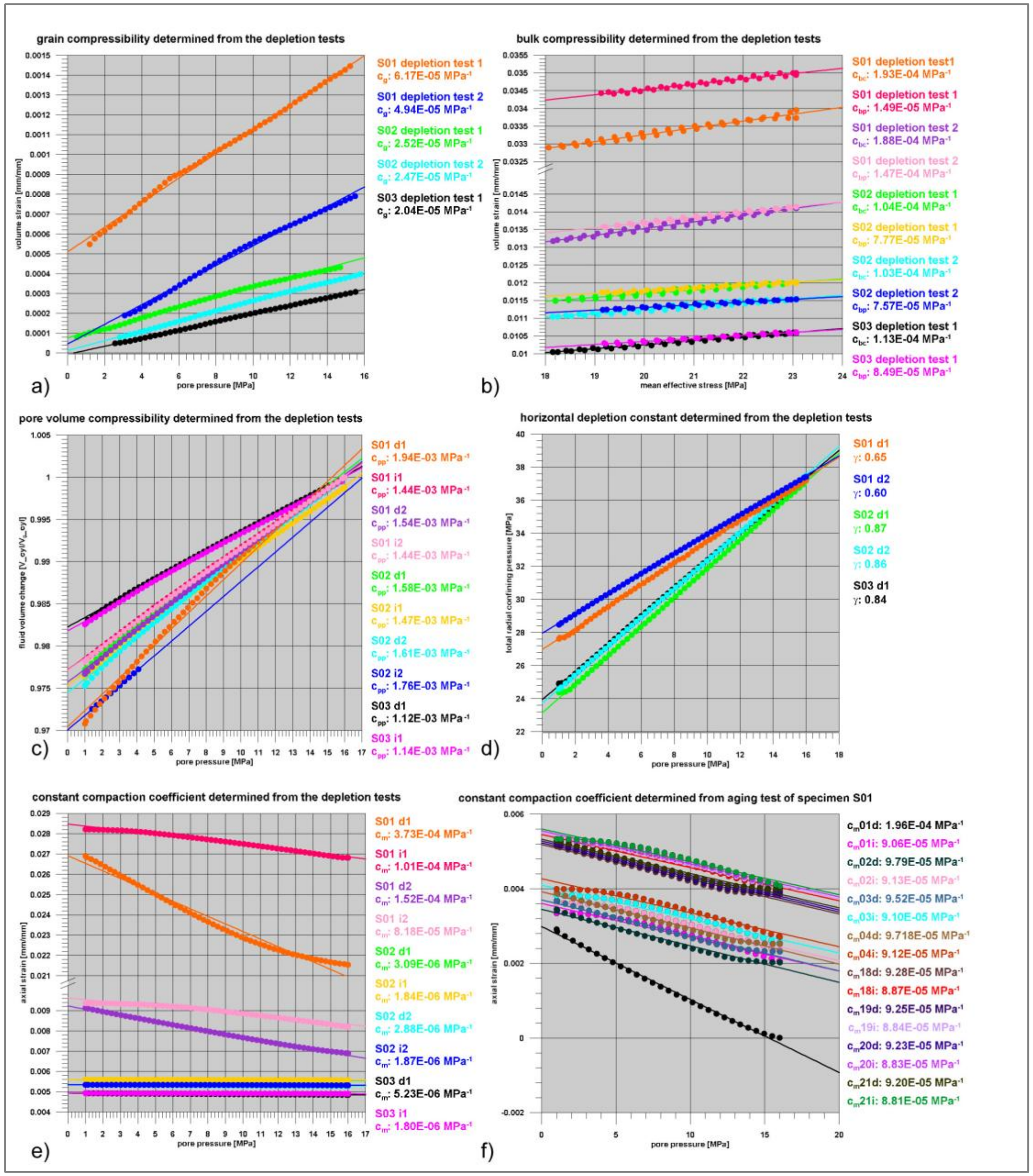

Figure 3. Poroelastic parameters, determined from the depletion tests (a-e) and the aging procedure (f): a) grain compressibility; b): bulk compressibility; c): pore volume compressibility; d): horizontal depletion constant; e): constant compaction coefficient; and f) constant compaction coefficient from several depletion/inflation cycles from the aging procedure of specimen S01.

Click to view slide presentation